Arch Toxicol (2015) 89:371–379
DOI 10.1007/s00204-014-1256-0

INORGANIC COMPOUNDS

A 13-week repeated-dose oral toxicity and bioaccumulation of aluminum oxide nanoparticles in mice

Eun-Jung Park · Jaehoon Sim · Younghun Kim · Beom Seok Han · Cheolho Yoon · Somin Lee · Myung-Haing Cho · Byoung-Seok Lee · Jae-Ho Kim

Received: 20 February 2014 / Accepted: 15 April 2014 / Published online: 6 May 2014

Abstract Because of an increase in the commercial applications of manufactured nanoparticles, the issue of potential adverse health effects of nanoparticles following intended or unintended exposure is rapidly gaining attention. In this study, we evaluated the toxicity of aluminum oxide nanoparticles (AlNPs, rod-type, 1.5, 3, and 6 mg/kg) after oral administration to mice for 13 weeks. Compared with the control group, the consumption of diet and drinking water and body weight gain decreased in the group treated with AlNPs. The group treated with 6 mg/kg AlNPs also showed a marked elevation in the count of white blood cells that associated with a significant decrease and increase to the proportion of eosinophils and lymphocytes, respectively. In addition, the secretion of IL-6 and monocyte chemotactic protein-1 increased in a dose-dependent manner in the treated groups. Furthermore, AlNPs showed the highest accumulation in the liver and kidneys compared with the control group, increased the lactate dehydrogenase level in the blood, and induced the development of a pathological lesion in the liver and kidneys. Taken together, we suggest that the target organs of rod-type AlNPs may be the liver, kidneys and the immune system, and the not-observed adverse effect level may be lower than 6 mg/kg.

Keywords Aluminum oxide nanoparticles · Toxicity · NOAEL · Eosinophils · Liver · Kidney

Electronic supplementary material The online version of this article (doi:10.1007/s00204-014-1256-0) contains supplementary material, which is available to authorized users.

E.-J. Park (✉) · J.-H. Kim
Department of Molecular Science and Technology, Ajou University, Suwon 443-749, Korea
e-mail: pejtoxic@hanmail.net

J. Sim · Y. Kim
Department of Chemical Engineering, Kwangwoon University, Seoul 139-701, Korea

B. S. Han
Hoseo Toxicological Research Center, Hoseo University, Asan 336-795, Korea

C. Yoon
Seoul Center, Korea Basic Science Institute, Seoul 126-16, Korea

S. Lee · M.-H. Cho
College of Veterinary Medicine, Seoul National University, Seoul 151-742, Korea

B.-S. Lee
Toxicologic Pathology Center, Korea Institute of Toxicology, Daejeon, Korea

Introduction

Typically, the size of manufactured nanomaterials (MNs) is in the range of 1–100 nm. MNs show novel properties compared with those of their macro-sized counterparts because of their unique structure. Although MNs are used in a broad range of sectors such as in medicine, environment, and energy production, the potential adverse effects of nanoparticles on humans and the environment because of unintended or intended exposure has attracted considerable attention. Thus, the Organization for Economic Co-operation and Development (OECD) launched a program in 2006 to assess the hazards, exposure, and risk associated with nanoparticles and listed 14 species of MNs belonging to the high-priority group in 2007 (www.oecd.org). Aluminum oxide nanoparticles (AlNPs) are one of them and have been widely used in many fields including electronics, dispersion-strengthening, nanocomposites, and drug

delivery (www.azonano.com; Morsy et al. 2013a; Meziani et al. 2009). However, the preliminary data about the toxicity of AlNPs are very limited.

Aluminum (Al) is the third most abundant element on earth and is a well-known environmental neurotoxin. Al overdose has been proposed to be associated with some neurodegenerative diseases in humans, such as Alzheimer's disease and Parkinsonism-dementia, for a long time, although the relationship between Al overdose and these diseases has not been clarified thus far (Miu and Benga 2006; Oyanagi 2005; Savory et al. 2006; Wu et al. 2012). Al also affected the activity of antioxidant enzymes, disturbed cellular metal homeostasis, especially that of iron (Wu et al. 2012; Kim et al. 2007; Middaugh et al. 2005; Ward et al. 2001), and increased the production of reactive oxygen species (ROS) (Khanna and Nehru 2007; Kumar et al. 2009). Similarly, AlNPs induced neurotoxicity via mitochondrial impairment and oxidative damage, resulting in neural cell loss (Dong et al. 2011; Chen et al. 2008; Zhang et al. 2011). In addition, Morsy et al. (2013a) reported that bioaccumulation of AlNPs depends on time, dose, and organ. In addition, the bioaccumulation of nanomaterials can be determined on the basis of the exposure route, because the properties of nanomaterials are altered by body fluids (Stebounova et al. 2011; Cho et al. 2011, 2013). In our previous study, we orally administered sphere type of AlNPs with a dose of 15, 30, and 60 mg/kg for 4 weeks (Park et al. 2011), but suspended AlNPs were unstable due to too high stock concentration (10,000 μg/mL). Also, the upper limit dose volume of 5 mL/kg is recommended in terms of animal welfare. Thus, we orally administered AlNPs to mice with a dose of 1.5, 3, and 6 mg/kg for 13 weeks (stock concentration: 1,000 μg/mL) in this study and investigated the bioaccumulation and toxic response following repeated administration of AlNPs. Furthermore, we examined the influence of AlNPs on homeostasis of some trace elements in the body.

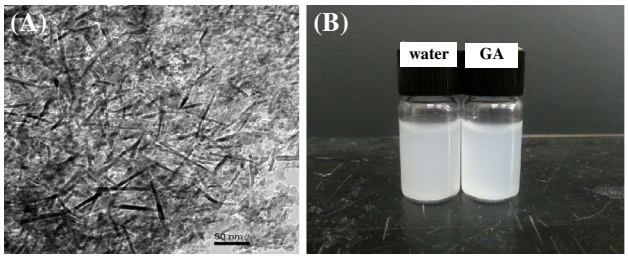

(C)

Solution	Diameter (nm)	Surface charge (mV)
Water	107.5 ± 30.9	72.44 ± 7.25
GA	92.9 ± 26.3	38.40 ± 1.35

Fig. 1 Characterization of AlNPs used in this study. Characterization of AlNPs was performed in drinking water and the artificial gastric juice (GA). **a** A TEM image (www.sigmaaldrich.com) indicates that AlNPs used in this study is rod type. **b** A picture of AlNPs in drinking water and the GA. **c** A summary of diameter and surface charge. AlNPs were suspended twice per week, and the measurement was performed twice, respectively, at the first and third day after suspension. The results represent mean ± standard deviation (SD) value

Materials and methods

AlNPs preparation and characterization

AlNPs were purchased from Sigma-Aldrich (Cat No. 544833, Fig. 1) and was dispersed at a concentration of 1 mg/ml in autoclaved drinking water using tip-type ultrasonifier (19 kHz, 30 min, Ulh700S). The size and surface charge of AlNPs was measured using the Zeta Potential and Particle Size Analyzer (ELSZ-2, Otsuka Electronics, Hirakata, Japan).

In vivo sample preparation

Six-week-old male ICR mice (27–28 g, OrientBio, Seongnam, Korea) were acclimatized for 1 week before the start of the study (IACUC No. 2012-0010) at constant temperature of 23 ± 3 °C, relative humidity of 50 ± 10 %, a 12-h light/dark cycle with a light of intensity 150–300 l×, and ventilation of 10–20 times/h. Temperature and relative humidity were monitored daily. After acclimation, AlNPs were administered orally at a dose of 1.5, 3 and 6 mg/kg for 13 weeks (n = 12/group, 6 times/week), and the control group was treated with autoclaved water. Beginning at Day 0, body weight was measured once in 14 days, and the consumption of drinking water and diets were measured once in 7 days. Blood (approximately 1.2 mL/mouse) was collected from the saphenous vein for the biochemical and hematological analysis as well as the cytokine assay, and then mice were killed. The brain, thymus, lung, heart, liver, kidneys, spleen, and testis were collected for measurement of metal ions in each tissue and for histological examinations.

Hematological and biochemical analysis

Hematological analyses of whole blood were conducted using a blood autoanalyzer (HemaVet850, CDC Tech. Co., USA). And, whole blood was centrifuged at 2,400g for 10 min to obtain serum for biochemical analysis, and serum was stored at −80 °C. Biochemical parameters including total protein, albumin, glucose, aspartate aminotransferase (AST), alanine aminotransferase (ALT), alkaline phosphatase (ALP), creatinine, BUN, γ-GTP, and lactate

dehydrogenase (LDH) were measured using an auto-analyzer (Hitachi 7180, Hitachi, Japan).

Metal ion measurement in tissue

Tissues were digested in a mixture of HNO_3 (70 %, 7 mL) and H_2O_2 (35 %, 1 mL) solution using a microwave digestion system (Milestone, Sorisole, Italy) under high temperature and pressure. Element concentration in lysates was measured using inductively coupled plasma mass spectrometry at the Korean Basic Science Institute (Supple 1, Park et al. 2014a, b).

Histopathological analysis

The kidneys and livers of control and treated group were fixed in 10 % neutral buffered formalin and processed using routine histological techniques. After paraffin embedding, 3-μm sections were cut and stained with hematoxylin and eosin (H&E) for histopathological examination by the light microscope.

Cytokine assay

The concentration of each cytokine (interleukin (IL)-1β, tumor necrosis factor alpha (TNF α), IL-6, transforming growth factor (TGF)-beta, granulocyte–macrophage colony-stimulating factor (GM–CSF), and monocyte chemotactic protein (MCP-1) was determined using commercially available enzyme-linked immunosorbent assay (ELISA) kits (eBioscience, Park et al. 2013). Briefly, each well in the 96-well plate was coated with 100 μL of capture antibody and incubated overnight at 4 °C. After blocking with assay diluents, the supernatant or standard antibody was added to each well, and the plates were maintained at RT for 2 h. After washing, biotin-conjugated detecting antibody was added to each well, and the plates were further incubated at RT for 1 h. Next, the plates were washed again and further incubated with avidin-horseradish peroxidase for 30 min. Finally, the reactions were stopped by adding 2N H_2SO_4, and the absorbance at 450 nm was measured using an ELISA reader (Molecular Devices). The concentration of each cytokine was calculated from the linear portion of the standard curve which was generated in the same condition.

Statistical analysis

Statistical analyses were performed using Student's *t* test (Graphpad Software, San Diego, CA, USA) and one way ANOVA test followed by Tukey's post hoc pairwise comparison. Asterisks (*) indicated statistically significant differences to the control group, $*p < 0.05$ and $**p < 0.01$.

Results

Characterization of AlNPs

According to the information from the manufacturing company, the raw AlNPs were of rod-type (Fig. 1a) with a size lower than 50 nm, and average surface area was greater than 40 m^2/g (www.sigmaaldrich.com). AlNPs were well dispersed in drinking water and the artificial gastric juice (GA, Marques et al. 2011, Fig. 1b). The hydrodynamic diameter of AlNPs was similar in between GA and drinking water, whereas the positive charge on surface was lower in the GA than drinking water (Fig. 1c, Supple 2).

Consumption of diet and drinking water

During the first week of the study, drinking water consumption per cage (4 mice/cage, 3 cages/group) in the groups treated with 1.5, 3 and 6 mg/kg AlNPs was 97.2 ± 6.2, 109.0 ± 4.0, and 100.9 ± 1.5 mL, respectively, whereas that in the control group was 129.5 ± 6.6 mL (Fig. 2a). Diet consumption per cage (4 mice/cage, 3 cages/group) in the groups treated with 1.5, 3, and 6 mg/kg AlNPs was 124.4 ± 4.3, 133.9 ± 4.3, and 128.0 ± 4.8 g, respectively and that in the control group was 135.6 ± 4.2 g (Fig. 2b). During the last week of the study, drinking water consumption per cage in the control group (0) and the groups treated with 1.5, 3, and 6 mg/kg AlNPs was 118.6 ± 11.1, 90.4 ± 8.5, 99.9 ± 4.7, and 92.7 ± 3.46 mL, respectively, and the corresponding diet consumption in these groups was 140.4 ± 8.7, 119.6 ± 7.0, 128.5 ± 12.6, and 113.5 ± 3.4 g, respectively.

Body weight changes

At the starting point of the study, the body weights of mice were 31.5 ± 0.4, 29.7 ± 1.0, 30.6 ± 0.7, and 30.1 ± 0.8 g in the control (0) and the groups treated with 1.5, 3 and 6 mg/kg AlNPs, respectively (Supple 3). The body weight measured before necropsy was also 45.3 ± 1.8, 42.0 ± 2.7, 42.5 ± 1.6, and 41.9 ± 1.4 g in the control (0), and 1.5, 3, and 6 mg/kg groups, respectively. Therefore, body weight gain in the groups treated with 1.5, 3, and 6 mg/kg AlNPs was 12.3 ± 1.7, 11.9 ± 0.8, 11.8 ± 0.8 g, respectively, whereas that in the control group was 13.8 ± 1.2 g (Fig. 3).

Hematological and biochemical changes

Biochemical changes in the blood after administration of AlNPs are shown in Table 1a. The levels of AST, ALT, and LDH were markedly different between the groups. Compared with the controls, the levels of AST, ALT, and LDH decreased in the mice treated with 1.5 and 3 mg/kg

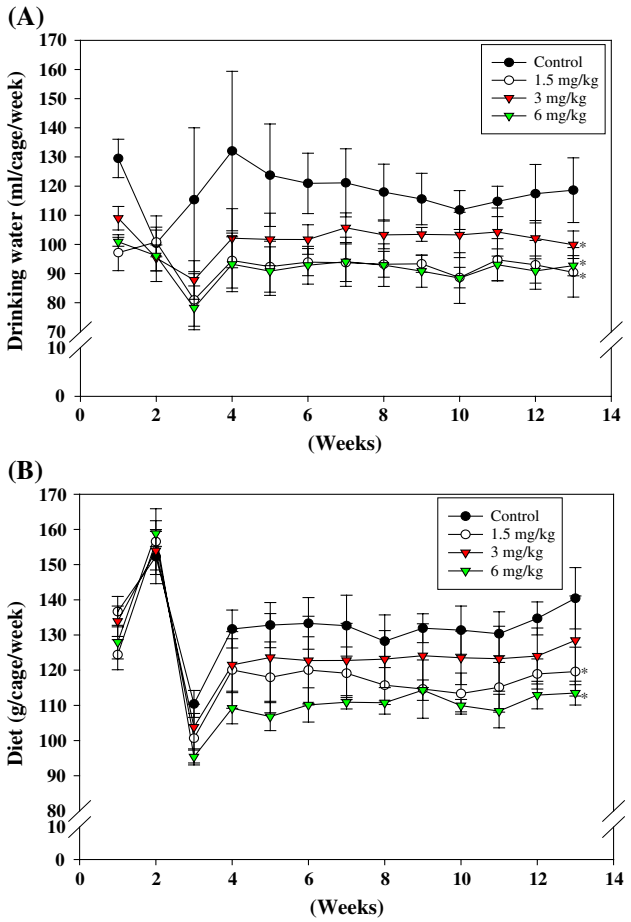

Fig. 2 Effect of AlNPs on consumption of drinking water and diet. Consumption of drinking water (**a**) and diet (**b**) per cage (4 mice/cage, 3 cages/group, $n = 3$) was measured once in 7 days, beginning at day 0. The results represent mean ± SD value; statistical significance was evaluated for the last week only; and asterisks indicate difference of the treated groups compared with the control group. $^*p < 0.05$

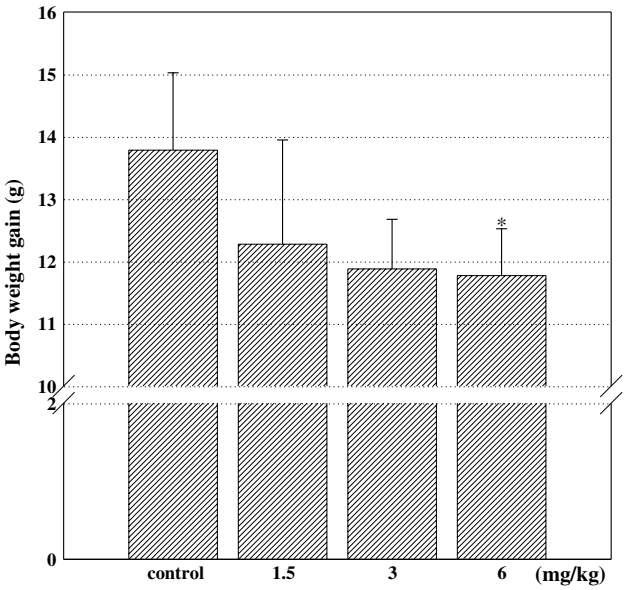

Fig. 3 Changes in body weight gain after repeated dose of AlNPs. Body weight was measured once in 14 days, beginning at day 0 ($n = 12$). The results represent mean ± SD value, and *asterisks* indicate difference of the treated groups compared with the control group at 13 weeks after administration. $^*p < 0.05$

AlNPs, but these levels were markedly elevated in the mice treated with 6 mg/kg AlNPs. In addition, the count of white blood cells (WBCs) and the proportion of lymphocytes in the WBCs significantly increased in the group treated with 6 mg/kg AlNPs compared with the control group, whereas the proportion of eosinophils in the WBCs markedly decreased in the group treated with 6 mg/kg AlNPs compared with the control group (Table 1b).

Distribution of Al and antioxidant elements in the tissues

The Al level in the tissues after repeated administration of AlNPs is shown in Table 2a. Comparing with the control group, the highest accumulation of Al was observed in the liver followed by the kidney, heart, lung, and thymus, whereas the Al level in the brain decreased. In addition, we measured the level of some trace elements in the body. Comparing with the control group, the level of manganese increased significantly in the brain (Table 2b), and the copper level increased in the heart, lung, testis, and thymus (Table 2c). Furthermore, the zinc (Table 2d) and iron level (Table 2e) were enhanced significantly in the thymus and the liver and lung at the highest dose, respectively. Meanwhile, the levels of copper and iron in the brain of the treated groups significantly decreased compared with those in the control group (Tables 2c, 3e).

Histopathological changes

We examined histopathological changes in the liver and kidney of the control and treated groups (Table 3, Supple 4). Dose-related histopathological lesions were observed in the liver and kidney of the mice treated with 6 mg/kg AlNPs.

Secretion of inflammatory cytokines

As shown in Fig. 4, the levels of IL-1β and TNF α in the treated groups did not change significantly compared with the corresponding levels in the control group, and GM–CSF and TGFβ were not detected at a significant level in all samples tested. However, the levels of IL-6 and MCP-1 increased in a dose-dependent manner. The levels of IL-6 were 16.6 ± 1.0, 23.4 ± 0.6, and 104.6 ± 0.6 pg/mL in the blood of the mice treated with 1.5, 3, and 6 mg/kg

Table 1 Changes in blood biochemistry after repeated dose of AlNPs

Unit	TP (g/dL)	ALB (g/dL)	T.Bil (mg/dL)	GLU (mg/dL)	BUN (mg/dL)	CREA (mg/dL)	AST (U/L)	ALT (U/L)	ALP (U/L)	r-GTP (U/L)	LDH (U/L)
a.											
Control	5.3 ± 0.5	2.9 ± 0.3	0.2 ± 0.0	193.7 ± 24.4	22.9 ± 1.9	0.3 ± 0.0	243.3 ± 22.3	232.7 ± 25.5	47.7 ± 3.1	0.0 ± 0.0	1,078.3 ± 49.0
1.5 mg/kg	5.4 ± 0.5	3.0 ± 0.2	0.2 ± 0.0	255 ± 39.4	18.0 ± 1.8*	0.3 ± 0.1	183.3 ± 80.9	154.8 ± 69.4	52.5 ± 6.1	0.3 ± 0.5	715.8 ± 304.5
3.0 mg/kg	5.7 ± 0.3	3.1 ± 0.2	0.2 ± 0.0	233.5 ± 48.8	18.4 ± 4.5	0.3 ± 0.0	123.8 ± 21.9	134.8 ± 36.0	58.0 ± 7.6	0.3 ± 0.5	499.5 ± 118.1*
6.0 mg/kg	5.2 ± 0.3	2.9 ± 0.2	0.2 ± 0.1	225.8 ± 64.3	20.6 ± 3.2	0.3 ± 0.1	495.3 ± 175.9*	749.8 ± 282.8*	47.5 ± 7.0	0.0 ± 0.0	2,430.5 ± 727.6*

Unit	WBC (K/uL)	LY (%)	MO (%)	NE (%)	EO (%)	BA (%)	RBC (M/uL)	MCV (fL)	HCT (%)	MCH (pg)	MCHC (g/dL)	Hgb (g/dL)	RDW (%)	PLT (K/uL)	MPV (fL)
b.															
Control	1.8 ± 0.2	80.9 ± 1.1	5.4 ± 0.3	9.8 ± 1.8	3.3 ± 0.9	0.6 ± 0.1	7.1 ± 0.5	55.6 ± 2.1	39.3 ± 4.0	13.4 ± 1.4	24.2 ± 1.6	9.5 ± 1.6	16.7 ± 0.4	936.5 ± 258.1	5.7 ± 0.2
1.5 mg/kg	2.9 ± 1.1	79.1 ± 5.3	5.3 ± 1.4	13.4 ± 5.5	1.8 ± 1.7	0.5 ± 0.1	7.1 ± 0.9	59.2 ± 1.7	41.9 ± 5.1	14.1 ± 0.6	23.9 ± 1.1	10.0 ± 0.9	16.1 ± 1.0	1,088.0 ± 208.7	5.7 ± 0.3
3.0 mg/kg	2.4 ± 0.3	87.4 ± 0.9*	3.0 ± 0.0	7.1 ± 1.6	2.2 ± 1.8	0.4 ± 0.1	7.7 ± 1.5	57.2 ± 4.1	43.8 ± 8.0	13.9 ± 0.6	24.3 ± 1.1	10.7 ± 2.2	16.6 ± 1.3	835.7 ± 235.7	6.0 ± 0.4
6.0 mg/kg	3.3 ± 1.2*	84.7 ± 2.6*	4.9 ± 1.0	9.1 ± 1.5	1.0 ± 0.6*	0.5 ± 0.1	6.8 ± 0.2	55.9 ± 0.9	37.9 ± 1.3	14.0 ± 0.7	25.0 ± 0.9	9.5 ± 0.6	16.7 ± 0.3	1,057.0 ± 75.4	5.8 ± 0.2

Results represent mean ± SD value. * $p < 0.05$. a Effect of AlNPs on biochemical parameters. Analysis was performed using four serum samples; serums from two mice were pooled to make one sample for analysis ($n = 4$), b effect of AlNPs on hematological parameters. Analysis was performed using whole blood from eight mice ($n = 8$)

Table 2 Effect of AlNPs on the distribution of trace elements in tissues

Al	Brain	Heart	Kidney	Spleen	Liver	Lung	Testis	Thymus
a.								
Control	4,859.4 ± 1,946.9	2,470.5 ± 385.1	1,487.0 ± 474.3	4,461.2 ± 1,316.1	1,581.2 ± 593.9	9,304.4 ± 117.4	5,059.2 ± 343.5	1,285.5 ± 123.1
1.5 mg/kg	3,111.3 ± 657.5	3,402.3 ± 338.0	2,244.9 ± 524.4	3,270.9 ± 139.6	4,329.3 ± 2,072.8	10,122.2 ± 822.7	2,849.5 ± 1,215.5	1,516.0 ± 102.4
3 mg/kg	2,612.2 ± 369.4	4,189.1 ± 989.0*	3,523.9 ± 1,153.9	2,865.5 ± 892.7	6,098.4 ± 4,495.4	19,190.9 ± 11,982.6	4,675.6 ± 500.3	1,904.7 ± 115.0*
6 mg/kg	2,185.0 ± 357.5*	7,112.0 ± 2,276.1*	4,623.3 ± 1,457.5*	3,713.3 ± 307.0	9,340.5 ± 3,901.1*	27,226.3 ± 11,996.0*	4,770.5 ± 18.1	2,367.5 ± 123.9*
Mn	Brain	Heart	Kidney	Spleen	Liver	Lung	Testis	Thymus
b.								
Control	416.2 ± 45.5	547.4 ± 774.1	1,247.2 ± 451.2	ND	771.7 ± 460.9	ND	86.5 ± 122.4	208.7 ± 13.5
1.5 mg/kg	508.3 ± 8.7*	519.5 ± 734.7	1,460.3 ± 682.6	ND	852.2 ± 456.1	ND	186.8 ± 11.7	184.4 ± 47.0
3 mg/kg	527.6 ± 25.3*	386.1 ± 546.1	1,254.5 ± 627.1	ND	883.3 ± 447.6	ND	171.6 ± 10.6	205.1 ± 15.6
6 mg/kg	547.5 ± 14.9*	515.8 ± 729.4	1,215.7 ± 478.8	ND	877.2 ± 459.4	ND	183.4 ± 80.4	183.7 ± 96.1
Cu	Brain	Heart	Kidney	Spleen	Liver	Lung	Testis	Thymus
c.								
Control	7,280.2 ± 1,877.5	4,730.9 ± 466.7	5,018.5 ± 1,076.0	5,177.6 ± 2,444.9	4,016.3 ± 1,237.4	3,012.0 ± 14.8	993.6 ± 17.9	2,038.2 ± 143.5
1.5 mg/kg	5,446.9 ± 2,153.9	5,160.0 ± 1,108.6	4,975.9 ± 674.7	2,884.9 ± 594.1	4,145.5 ± 1,803.5	2,721.9 ± 202.1	1,213.7 ± 20.7*	1,967.2 ± 62.4
3 mg/kg	4,403.7 ± 1,236.9	4,804.5 ± 732.8	4,155.4 ± 1,466.0	1,584.7 ± 403.8*	4,946.2 ± 2,094.5	3,142.2 ± 391.4	1,585.8 ± 273.7*	2,219.6 ± 249.2
6 mg/kg	4,046.5 ± 1,279.3*	6,364.1 ± 538.8*	4,066.6 ± 1,229.2	1,197.2 ± 40.9*	5,967.9 ± 3,138.4	4,327.4 ± 995.2*	1,418.6 ± 34.9*	2,385.3 ± 124.9*
Zn	Brain	Heart	Kidney	Spleen	Liver	Lung	Testis	Thymus
d.								
Control	6,968.4 ± 650.4	7,803.4 ± 214.9	13,509.4 ± 8,003.9	12,826.6 ± 2,467.5	15,900.7 ± 750.1	10,227.7 ± 628.4	11,248.0 ± 447.0	11,277.8 ± 647.3
1.5 mg/kg	7,938.2 ± 1,109.5	7,847.9 ± 1,524.3	10,420.3 ± 1,048.9	11,204.8 ± 245.7	15,995.9 ± 790.9	9,496.7 ± 340.9	10,938.2 ± 20.5	12,058.9 ± 960.9
3 mg/kg	7,149.5 ± 994.5	7,751.3 ± 299.8	9,038.6 ± 606.4	10,975.0 ± 355.4	17,258.4 ± 283.4	11,025.2 ± 2,122.0	23,004.2 ± 15,783.7	12,364.1 ± 1,034.4
6 mg/kg	7,093.8 ± 180.5	8,478.4 ± 635.7	9,538.5 ± 800.6	10,559.1 ± 489.0	17,673.7 ± 903.6	9,548.5 ± 526.0	11,520.1 ± 149.1	13,635.8 ± 728.9*
Fe	Brain	Heart	Kidney	Spleen	Liver	Lung	Testis	Thymus
e.								
Control	26,921.9 ± 3,002.3	55,354.6 ± 2,182.0	43,664.6 ± 6,295.9	464,647.1 ± 173,277.5	74,600.1 ± 1,792.2	78,132.7 ± 3,944.8	17,767.9 ± 526.4	90,976.6 ± 2,497.6
1.5 mg/kg	18,385.1 ± 7,033.0	58,940.4 ± 7,796.9	44,665.7 ± 2,225.2	353,176.3 ± 46,013.2	83,472.1 ± 8,005.3	82,477.8 ± 529.2	17,519.2 ± 1,908.4	94,218.2 ± 6,089.5
3 mg/kg	17,435.1 ± 7,182.0	57,802.2 ± 1,804.8	42,709.6 ± 4,391.0	365,793.0 ± 173,991.3	104,149.0 ± 19,371.4*	88,047.5 ± 2,528.7*	18,607.6 ± 1,519.7	90,713.9 ± 4,881.6
6 mg/kg	16,349.9 ± 6,757.3*	66,309.4 ± 5,095.3*	42,070.4 ± 7,854.0	401,493.1 ± 5,163.9	159,759.3 ± 38,087.2*	91,025.5 ± 4,211.5*	19,756.5 ± 1,415.1	103,796.0 ± 5,434.0

Tissues from 4 mice were pooled for one analysis. Each tissue was digested in a mixture of HNO_3 (70 %) and H_2O_2 (30 %) solution using a microwave digestion system, under high temperature and pressure. Results represent mean ± SD value ($n = 3$). * $p < 0.05$. (A) Al, (B) manganese (Mn), (C) Cupper (Cu), (D) Zinc (Zn), and (E) iron (Fe)

Table 3 Histopathological changes following repeated dose of AlNPs

	Liver	Kidney
Control		
1	NHL	NHL
2	NHL	NHL
3	Vacuolation, diffuse, severe	NHL
4	NHL	NHL
1.5 mg/kg		
1	NHL	NHL
2	NHL	Tubular vacuolation, minimal
3	NHL	NHL
4	NHL	NHL
3 mg/kg		
1	NP accumulation, mild	NHL
2	NHL	NHL
3	NHL	NHL
4	Hypertrophy	NHL
6 mg/kg		
1	NHL	NHL
2	NP accumulation, minimal	Tubular vacuolation, mild
3	Chronic inflammation, moderate, necrosis, mild	Tubular vacuolation, mild
4	NHL	NHL

NHL no histological lesion

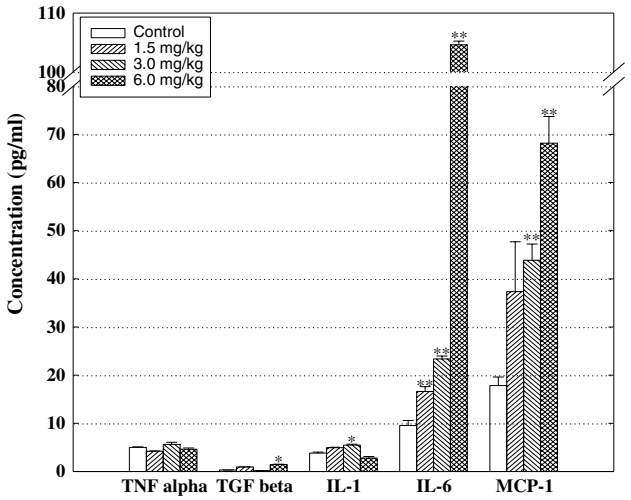

Fig. 4 Changes in the cytokine secretions after repeated dose of AlNPs. The experiment was performed using six serum sample ($n = 6$), and standard curve was made by a serial dilution from blank to 500 pg/mL. The results represent mean ± SD value. *$p < 0.05$, **$p < 0.01$

AlNPs, respectively, whereas that in the control group was 9.5 ± 1.0 pg/mL. In addition, the levels of MCP-1 were 17.9 ± 1.8, 37.4 ± 10.4, 43.9 ± 3.5, and 68.2 ± 5.6 pg/mL in the control (0), and 1.5, 3, and 6 mg/kg groups, respectively.

Discussion

Repeated-dose toxicity test is one of the most essential tests for the development and commercialization of products, and the main objectives of repeated-dose toxicity test is to calculate the not-observed adverse effect levels (NOAELs) and to determine whether one or more organ or system is adversely affected after 1- or 3-month exposure to nanoparticles. And, consumption of diet and drinking water and body weight changes are among the most essential endpoints in repeated-dose toxicity test. In addition, since the interactions between the MNs and biological organisms typically occur at the surface of the nanoparticle, the surface characteristics of nanomaterials are of great importance in determining their possible toxic effects (Jia et al. 2005; Wagner et al. 2007). In a previous study, we used AlNPs by Degussa (NRW, Germany, Park et al. 2011). These AlNPs were spherical in shape (hereafter, sphere-type AlNPs), and their hydrodynamic diameter and surface charge in deionized water (DW) and gastric juice were similar to those of rod-type AlNPs used in this study (Supple 5). Compared with the control group, the group treated with sphere-type AlNPs (15, 30, and 60 mg/kg daily) orally for 4 weeks showed a significant decrease in body weight gain despite an increase in the consumption of diet and drinking water. However, oral administration of rod-type AlNPs (1.5, 3, and 6 mg/kg, 6 times/week) for 13 weeks caused a decrease in the consumption of drinking water and diet and body weight gain (Supple 6).

Braydich-Stolle et al. (2010) reported that AlNPs impaired the natural ability of the cell to respond to a respiratory pathogen by altering the immune function. In our previous study, sphere-type AlNPs decreased both the count of WBCs and the proportion of neutrophils, monocytes, and lymphocytes (Park et al. 2011). However, in this study, the number of WBCs and the proportion of lymphocytes increased in the mice treated with 6 mg/kg AlNPs (rod-type), whereas the proportion of eosinophils decreased in a dose-dependent manner. Eosinophils are "acid-loving" and control mechanisms associated with allergy and asthma (Wardlaw 1994). Considering that AlNPs are amphoteric, which neutralize the other and produce a salt, we hypothesize that a decrease in the proportion of eosinophils following repeated administration of AlNPs may be because of the neutralizing ability of AlNPs (Hem et al. 1982).

Additionally, in this study, the LDH levels significantly increased in the blood of mice treated with 6 mg/kg of AlNPs. LDH is a cytoplasmic enzyme that converts pyruvate, the final product of glycolysis, to lactate in the

absence of or during a short supply of oxygen; therefore, an increase in the LDH level indicates damage of the cell membrane by toxicants.

Also, AlNPs injected through the peritoneum in a single acute doses (3.9, 6.4, and 8.5 g/kg) showed the highest accumulation in the spleen followed by the kidney, brain, intestine, and liver, whereas AlNPs injected at a sublethal dose (1.3 g/kg) once in 2 days for 28 days showed the highest accumulation in the liver followed by the spleen, intestine, kidney, and brain (Morsy et al. 2013a, b). Additionally, sphere-type AlNPs (15, 30, and 60 mg/kg), which are administered orally for 4 weeks, accumulated in the brain, thymus, and lung accompanying release from liver (Park et al. 2011). In this study, the AlNPs (rod-type) accumulated in the liver (5.9-fold), kidney (3.1-fold), lung (2.9-fold), and heart (2.9-fold) and were released from the brain. Furthermore, the tissue samples examined in the previous study (sphere-type) did not show any histopathological lesions, whereas, in this study, dose-related histopathological lesions were observed in the liver and kidney of the mice treated with 6 mg/kg of AlNPs (rod type). The shape of nanomaterials is as important as size in determining the toxicity of nanoparticles (Almeida et al. 2011; Perry et al. 2011; Tarantola et al. 2011), and the excretion rate of rod-type was markedly lower than that of sphere-type (Sun et al. 2011). Therefore, we believe that an increase in the LDH levels (6 mg/kg) may be attributed to cell membrane damage following the accumulation of AlNPs (Supple 7) and that further studies are required to determine the relationship between the shape of AlNPs and toxicity.

Furthermore, some researchers reported that AlNPs induced toxicity by enhancing the intracellular ROS levels (Prabhakar et al. 2012; Dong et al. 2011). Superoxide dismutases (SOD) are important antioxidant enzymes that guard against superoxide toxicity, and SOD enzymes employ either a copper, zinc or manganese as cofactor to carry out the disproportionation of SOD (Cullotta et al. 2006). Al also disturbed cellular metal homeostasis, especially that of iron (Wu et al. 2012; Kim et al. 2007; Middaugh et al. 2005; Ward et al. 2001). Thus, we determined the levels of copper, zinc, manganese, and iron with the Al level in the tissues of mice. Interestingly, the levels of these trace elements increased in the liver as the Al level. Also, the copper and iron levels decreased in the brain as the Al level. However, the manganese level increased in a dose-dependent manner in the brain. In our previous study, the expressions of neurodegeneration-related genes, including solute carrier family 6, tryptophan hydroxylase 2, and transcription factor AP-2 beta, were significantly up-regulated in the mice injected with 60 mg/kg of sphere-type AlNPs (Park et al. 2011). Herein, we feel the need of further study for the relationship between ion balance in the brain after administration of AlNPs and the development of neurological disease (Ward et al. 2001; Middaugh et al. 2005; Oyanagi 2005). Furthermore, the level of iron increased in the liver, lung, and heart as the Al level. Iron is an essential element in cellular energy metabolism, although excess iron can induce oxidative stress followed by cell death (Oexle et al. 1999; Gille and Reichmann 2011; Park et al. 2014b; Núñez et al. 2012). Therefore, we hypothesize that the increase in the iron level in this study may attribute to energy supplement for the regeneration of cells in damaged tissues.

Finally, cytokines and chemokines are extracellular proteins, which lead to migration of immune cells to the damaged sites. In this study, the levels of IL-6 and MCP-1 increased in a dose-dependent manner in the mice treated with AlNPs. However, the level of GM–CSF did not change after treatment with AlNPs. IL-6 is secreted by T cells and macrophages in an immune response for tissue damage, and MCP-1 recruits monocytes, T cells, and dendritic cells to the sites of inflammation produced by tissue injury (Zimmermann et al. 2012; Stinghen et al. 2010; Deshmane et al. 2009). In addition, eosinophils develop and mature in the bone marrow and differentiate in response to cytokines such as IL-3, IL-5, and GM–CSF. Furthermore, eosinopenia, which is a decrease in the number of eosinophil granulocytes, is often related to acute inflammation or stress (Wardlaw 1994).

Taken together, our results suggest that the target organs for accumulation of rod-type of AlNPs are the liver and kidney as well as the immune system, and the NOAEL of rod-type AlNPs may be lower than 6 mg/kg. In addition, further studies are required to address the potential possibility of eosinopenia after exposure to AlNPs.

Acknowledgments This work was supported by the Basic Science Research Program through the National Research Foundation of Korea funded by the Ministry of Education, Science, and Technology (2011-35B-E00011).

Conflict of interest The authors report no conflicts of interest.

References

Almeida JP, Chen AL, Foster A, Drezek R (2011) In vivo biodistribution of nanoparticles. Nanomedicine (Lond) 6(5):815–835

Braydich-Stolle LK, Speshock JL, Castle A, Smith M, Murdock RC, Hussain SM (2010) Nanosized aluminum altered immune function. ACS Nano 4(7):3661–3670

Chen L, Yokel RA, Hennig B, Toborek M (2008) Manufactured aluminum oxide nanoparticles decrease expression of tight junction proteins in brain vasculature. J Neuroimmune Pharmacol 3(4):286–295

Cho WS, Duffin R, Howie SE, Scotton CJ, Wallace WA, Macnee W, Bradley M, Megson IL, Donaldson K (2011) Progressive severe lung injury by zinc oxide nanoparticles; the role of Zn2 + dissolution inside lysosomes. Part Fibre Toxicol 8:27

Cho WS, Kang BC, Lee JK, Jeong J, Che JH, Seok SH (2013) Comparative absorption, distribution, and excretion of titanium dioxide and zinc oxide nanoparticles after repeated oral administration. Part Fibre Toxicol 10:9

Cullotta VC, Yang M, O'Halloran TV (2006) Activation of superoxide dismutases: putting the metal to the pedal. Biochim Biophys Acta 1763(7):747–758

Deshmane SL, Kremlev S, Amini S, Sawaya BE (2009) Monocyte chemoattractant protein-1 (MCP-1): an overview. J Interfer Cytokine Res 29(6):313–326

Dong E, Wang Y, Yang ST, Yuan Y, Nie H, Chang Y, Wang L, Liu Y, Wang H (2011) Toxicity of nano gamma alumina to neural stem cells. J Nanosci Nanotechnol 11(9):7848–7856

Gille G, Reichmann H (2011) Iron-dependent functions of mitochondria—relation to neurodegeneration. J Neural Transm 118(3):349–359

http://www.sigmaaldrich.com/catalog/product/aldrich/544833

Hem SL, White JL, Buehler JD, Luber JR, Grim WM, Lipka EA (1982) Evaluation of antacid suspensions containing aluminum hydroxide and magnesium hydroxide. Am J Hosp Pharm 39(11):1925–1930

Jia G, Wang H, Yan L, Wang X, Pei R, Yan T, Zhao Y, Guo X (2005) Cytotoxicity of carbon nanomaterials: single-wall nanotube, multi-wall nanotube, and fullerene. Environ Sci Technol 39(5):1378–1383

Khanna P, Nehru B (2007) Antioxidant enzymatic system in neuronal and glial cells enriched fractions of rat brain after aluminum exposure. Cell Mol Neurobiol 27(7):959–969

Kim Y, Olivi L, Cheong JH, Maertens A, Bressler JP (2007) Aluminium stimulates uptake of non-transferrin bound iron and transferrin bound iron in human glial cells. Toxicol Appl Pharmacol 220(3):349–356

Kumar V, Bal A, Gill KD (2009) Susceptibility of mitochondrial superoxide dismutase to aluminium induced oxidative damage. Toxicology 255(3):117–123

Marques MRC, Loebenberg R, Almukainzi M (2011) Simulated biological fluids with possible application in dissolution testing. Dissolut Technol 8:15–28

Meziani MJ, Bunker CE, Lu F, Li H, Wang W, Guliants EA, Quinn RA, Sun YP (2009) Formation and properties of stabilized aluminum nanoparticles. ACS Appl Mater Interfaces 1(3):703–709

Middaugh J, Hamel R, Jean-Baptiste G, Beriault R, Chenier D, Appanna VD (2005) Aluminum triggers decreased aconitase activity via Fe-S cluster disruption and the overexpression of isocitrate dehydrogenase and isocitrate lyase: a metabolic network mediating cellular survival. J Biol Chem 280(5):3159–3165

Miu AC, Benga O (2006) Aluminum and Alzheimer's disease: a new look. J Alzheimers Dis 10(2–3):179–201

Morsy GM, Abou El-Ala KS, Ali AA (2013a) Studies on fate and toxicity of nanoalumina in male albino rats: oxidative stress in the brain, liver and kidney. Toxicol Ind Health (epub ahead of print)

Morsy GM, Abou El-Ala KS, Ali AA (2013b) Studies on fate and toxicity of nanoalumina in male albino rats: lethality, bioaccumulation and genotoxicity. Toxicol Ind Health (epub ahead of print)

Núñez MT, Urrutia P, Mena N, Aguirre P, Tapia V, Salazar J (2012) Iron toxicity in neurodegeneration. Biometals 25(4):761–776

Oexle H, Gnaiger E, Weiss G (1999) Iron-dependent changes in cellular energy metabolism: influence on citric acid cycle and oxidative phosphorylation. Biochim Biophys Acta 1413(3):99–107

Oyanagi K (2005) The nature of the parkinsonism-dementia complex and amyotrophic lateral sclerosis of Guam and magnesium deficiency. Parkinsonism Relat Disord 11(Suppl 1):S17–S23

Park EJ, Kim H, Kim Y, Choi K (2011) Repeated-dose toxicity attributed to aluminum nanoparticles following 28-day oral administration, particularly on gene expression in mouse brain. Toxicol Environ Chem 93(1):120–133

Park EJ, Shim HW, Lee GH, Kim JH, Kim DW (2013) Comparison of toxicity between the different-type TiO_2 nanowires in vivo and in vitro. Arch Toxicol 87(7):1219–1230

Park EJ, Zahari NE, Lee EW, Song J, Lee JH, Cho MH, Kim JH (2014a) SWCNTs induced autophagic cell death in human bronchial epithelial cells. Toxicol In Vitro 28(3):442–450

Park EJ, Umh HN, Kim SW, Cho MH, Kim JH, Kim Y (2014b) ERK pathway is activated in bare-FeNPs-induced autophagy. Arch Toxicol 88(2):323–336

Perry JL, Herlihy KP, Napier ME, Desimone JM (2011) PRINT: a novel platform toward shape and size specific nanoparticle theranostics. Acc Chem Res 44(10):990–998

Prabhakar PV, Reddy UA, Singh SP, Balasubramanyam A, Rahman MF, Indu Kumari S, Agawane SB, Murty US, Grover P, Mahboob M (2012) Oxidative stress induced by aluminum oxide nanomaterials after acute oral treatment in Wistar rats. J Appl Toxicol 32(6):436–445

Savory J, Herman MM, Ghribi O (2006) Mechanisms of aluminum-induced neurodegeneration in animals: implications for Alzheimer's disease. J Alzheimers Dis 10(2–3):135–144

Stebounova LV, Guio E, Grassian VH (2011) Silver nanoparticles in simulated biological media: a study of aggregation, sedimentation, and dissolution. J Nanopart Res 13:233–244

Stinghen AE, Bucharles S, Riella MC, Pecoits-Filho R (2010) Immune mechanisms involved in cardiovascular complications of chronic kidney disease. Blood Purif 29(2):114–120

Sun YN, Wang CD, Zhang XM, Ren L, Tian XH (2011) Shape dependence of gold nanoparticles on in vivo acute toxicological effects and biodistribution. J Nano Sci Nanotechnol 11(2):1210–1216

Tarantola M, Pietuch A, Schneider D, Rother J, Sunnick E, Rosman C, Pierrat S, Sönnichsen C, Wegener J, Janshoff A (2011) Toxicity of gold-nanoparticles: synergistic effects of shape and surface functionalization on micromotility of epithelial cells. Nanotoxicology 5(2):254–268

Wagner AJ, Bleckmann CA, Murdock RC, Schrand AM, Schlager JJ, Hussain SM (2007) Cellular interaction of different forms of aluminum nanoparticles in rat alveolar macrophages. J Phys Chem B 111(25):7353–7359

Ward RJ, Zhang Y, Crichton RR (2001) Aluminium toxicity and iron homeostasis. J Inorg Biochem 87(1–2):9–14

Wardlaw AJ (1994) Eosinophils in the 1990s: new perspectives on their role in health and disease. Postgrad Med J 70(826):536–552

Wu Z, Du Y, Xue H, Wu Y, Zhou B (2012) Aluminum induces neurodegeneration and its toxicity arises from increased iron accumulation and reactive oxygen species (ROS) production. Neurobiol Aging 33(1):199.e1–e12

www.oecd.org. 2012. Six years of OECD work on the safety of manufactured nanomaterials: Achievements and future opportunities

Zhang QL, Li MQ, Ji JW, Gao FP, Bai R, Chen CY, Wang ZW, Zhang C, Niu Q (2011) In vivo toxicity of nano-alumina on mice neurobehavioral profiles and the potential mechanisms. Int J Immunopathol Pharmacol 24(1 Suppl):23S–29S

Zimmermann HW, Trautwein C, Tacke F (2012) Functional role of monocytes and macrophages for the inflammatory response in acute liver injury. Front Physiol 3:56